



HAL
open science

Investigation of the electrical limit conditions effects in piezoelectric transducer arrays utilized in medical imaging

Imane Laasri, Abdelmajid Bybi, Ouadia Mouhat, Mohammad Jamal, Anne-Christine Hladky, Aziz Ettahir, Kamal Kettani

► To cite this version:

Imane Laasri, Abdelmajid Bybi, Ouadia Mouhat, Mohammad Jamal, Anne-Christine Hladky, et al.. Investigation of the electrical limit conditions effects in piezoelectric transducer arrays utilized in medical imaging. *Applied Acoustics*, 2020, 10.1016/j.apacoust.2020.107509 . hal-03019835

HAL Id: hal-03019835

<https://hal.science/hal-03019835v1>

Submitted on 7 Dec 2020

HAL is a multi-disciplinary open access archive for the deposit and dissemination of scientific research documents, whether they are published or not. The documents may come from teaching and research institutions in France or abroad, or from public or private research centers.

L'archive ouverte pluridisciplinaire **HAL**, est destinée au dépôt et à la diffusion de documents scientifiques de niveau recherche, publiés ou non, émanant des établissements d'enseignement et de recherche français ou étrangers, des laboratoires publics ou privés.

Investigation of the electrical limit conditions effects in piezoelectric transducer arrays utilized in medical imaging

Imane LAASRI¹, Abdelmajid BYBI^{2*}, Ouadia MOUHAT³, Mohammad JAMAL¹, Anne Christine HLADKY⁴, Aziz ETTAHIR², and Kamal KETTANI²

¹Hassan II University of Casablanca, Faculty of Sciences Ben M'sik, Department of Physics, Engineering and Materials Laboratory (LIMAT), Engineering and Mechanics Team.

^{2,3}Mohammed V University in Rabat, Ecole Supérieure de Technologie de Salé

²MEAT - Materials Energy and Acoustics Team

³LGCE - Laboratoire Génie Civil et Environnement

⁴Univ. Lille, CNRS, Centrale Lille, ISEN, UPHF, UMR 8520, IEMN Lille, France

* Corresponding author: abdelmajid.bybi@um5.ac.ma

Ecole Supérieure de Technologie de Salé
Avenue Le Prince Héritier, B.P 227, 11000 Salé Médina. Maroc

Abstract

Crosstalk is considered as an undesirable phenomenon disturbing the electromechanical behavior of the ultrasonic transducer arrays used in medical imaging applications. Indeed, when one element of a transducer array is excited, it generates parasitic voltages and/or displacement fields on the adjacent passive elements. Consequently, these interactions between elements decrease the array's electroacoustic performance, which affects the obtained image quality. To overcome the crosstalk's problem, several research works propose active cancellation techniques. In this case, the correction voltages are determined by considering the array's elements grounded, contrary to the conventional crosstalk's definition which considers the array elements in Open-Circuit. The novelty of this paper is in one hand the study of the electrical limit conditions' effects on the physical behavior of a piezoelectric transducer array radiating in a fluid medium (water). On the other hand, a displacement method is proposed to evaluate the crosstalk level when the array elements are grounded. The limitations of the proposed method are also discussed. For this purpose, a piezoelectric transducer array is firstly modeled using a Two-dimensional Finite Elements Method (FEM), when the array elements are not grounded (open-circuit). Then, the results are compared to those obtained when the neighboring elements are grounded (as in the case of the crosstalk's active cancellation techniques).

34 Finally, measurements are realized on a fabricated transducer array vibrating in air medium and are
35 successfully compared to the results predicted using FEM.

36 *Keywords—Piezoelectric transducer arrays, displacement measurement, electrical limit conditions.*

37

38 ***1. Introduction***

39 Ultrasonic transducers and transducer arrays are usually utilized in medical diagnostics
40 and therapeutic applications [1-5]. The major objective of ongoing and future research in this
41 area is to optimize the electroacoustic performance of these transducers, to obtain a high image
42 resolution for more reliable and safe diagnostics. For this purpose, several works investigate
43 the crosstalk phenomenon, which decreases the performance of the ultrasonic transducer arrays
44 [6-14]. Indeed, when one element of a transducer array is driven, it generates parasitic voltages
45 and/or displacement fields on the passive neighboring elements, which affects the performance
46 of these devices. It is mainly responsible for anomalous behavior in the directivity of the
47 ultrasonic transducer arrays, i.e. in presence of crosstalk, the main lobe is not obtained in the
48 axial direction of the transducer array and several undesirable side lobes can be observed [15-
49 16]. The crosstalk level in the ultrasonic transducer arrays is generally evaluated as the ratio
50 between the parasitic voltages obtained on the passive neighboring elements and the
51 excitation's amplitude applied to the active element [11, 14]. In this definition, one element of
52 the studied transducer array is electrically driven, while its neighboring elements are
53 considered electrically in Open-Circuit (not grounded).

54 In literature research works devoted to the minimization of crosstalk can be divided into
55 three approaches. The first one investigates the contribution of the passive elements, i.e.
56 filling material, matching layers, and backing, to the mechanical crosstalk [17-21]. The
57 second approach consists of developing a systematic method for the active cancellation of
58 crosstalk. The last method concerns specific treatments realized on the excitation and
59 reception signals to reduce crosstalk [22-23]. The active cancellation of crosstalk is based on
60 the application of adequate voltages to the elements adjacent to the excited one, to minimize
61 the parasitic signals (crosstalk). The required voltages can be determined using different
62 methods. Cugnet et al. [24] proposed a numerical technique to calculate them from the
63 average normal displacement computed at the surface of the array elements. In the same
64 manner, Bybi et al. [16] determined the correction voltages from punctual displacement
65 measurements realized using a Laser Vibrometer. Zhou et al. [25-26] developed another

66 method using the transfer function matrix relating input voltages V_i to output pressures P_i . In
67 this case, the measurement of the elements transfer function is realized using a hydrophone.
68 Finally, Bybi et al. [7, 27] proposed another simple electrical method to cancel crosstalk in
69 acoustical arrays, using the analogy between the motional current and normal displacement.
70 In this situation, the determination of the correction voltages requires average measurements,
71 i.e. impedance and current measurements, instead of punctual displacement measurements.

72 In all active crosstalk cancellation techniques, the determination of the correction
73 voltages considers the neighboring elements electrically in Short-Circuit, i.e. the passive
74 neighboring elements are connected to the ground, contrary to the conventional definition
75 (neighboring elements are not grounded). The main objective of this paper is to study the
76 effects of the electrical limit conditions (neighboring elements grounded or not grounded) on
77 the electromechanical behavior of the piezoelectric transducer arrays utilized in medical
78 imaging. An alternative solution to the conventional crosstalk's evaluation method, i.e. based
79 on the ratio between the parasitic voltages measured on each passive element and the
80 excitation voltage, is also proposed and tested when the array elements are grounded. It is
81 expected that this study will be helpful in terms of crosstalk definition and accurate evaluation
82 and suppression.

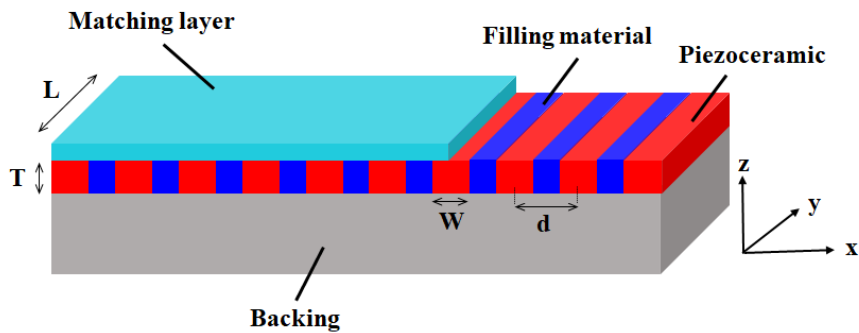
83 The first part of this paper is devoted to the description of a conventional piezoelectric
84 transducer array and the presentation of the experimental setup utilized to evaluate the
85 crosstalk level. In the second part, a transducer array composed of seven piezoelectric elements
86 made of PZ 27 ceramic is modeled using a two-dimensional finite element method. In the last
87 section, a prototype is fabricated and the experimental results, i.e. electrical impedance and
88 displacement curves are compared to the numerical ones (FEM). Finally, the crosstalk level is
89 evaluated experimentally considering both electrical limit conditions: neighboring elements
90 ground and not grounded.

91 **2. Piezoelectric transducer arrays for medical imaging applications**

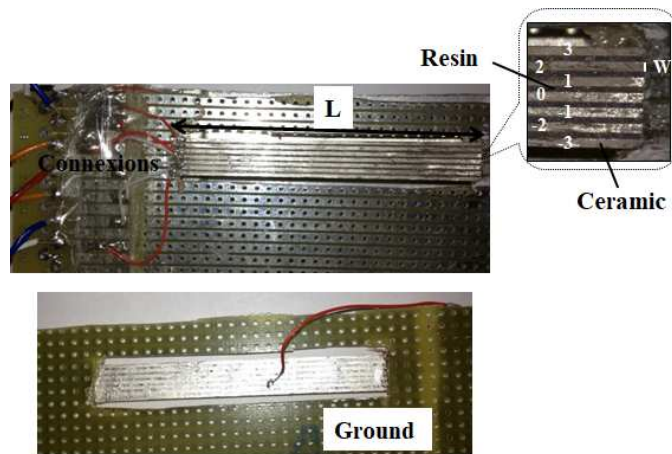
92 **2.1 Structure description**

93 Transducer arrays utilized in medical imaging and NDT applications are generally
94 composed of an even number of piezoelectric elements having a thickness T , a width W , and a
95 length L , spaced by a distance d and aligned as illustrated in Fig. 1. The elements are
96 polarized in the thickness direction (z -direction) and are bonded to each other by a non-
97 conductive resin. The transducer array elements' are also equipped with front and back

98 matching layers, to minimize the mismatching problem, which creates a prolonged ringing
 99 after pulse excitation. Generally, the acoustic impedance of a conventional transducer is
 100 matched to that of the propagation medium (tissues in medical applications) by one or two
 101 matching layers on its front face and a thick backing layer on its back face. In our study, the
 102 manufactured array is only composed of piezoelectric elements bonded to each other by a
 103 non-conductive acrylic resin, PLEXCIL (ESCIL). The matching layers are not taken into
 104 account to facilitate the fabrication of the prototype. This kind of transducer arrays is utilized
 105 to understand the crosstalk phenomenon and to study the effects of the electrical limit
 106 conditions on the array's electromechanical behavior. This also allowed as testing our
 107 crosstalk correction methods easily [16, 27].



108
 109 **Figure 1:** Schematic description of a conventional piezoelectric transducer array.



110
 111 **Figure 2:** Seven-element transducer array.

112 To get a full symmetry of the transducer array and to simplify calculations and analysis,
 113 an odd number of transducers is assumed. As shown in Fig. 2, the fabricated prototype is
 114 composed of seven piezoelectric elements made of PZ27 Ferroperm ceramic, having the
 115 following dimensions: $T = 3.3$ mm, $W = 0.7$ mm, $L = 37$ mm and $d = 1.2$ mm. The
 116 piezoelectric material (PZ27) properties are listed in Table I.

S_{11}^E pPa ⁻¹	S_{12}^E pPa ⁻¹	S_{13}^E pPa ⁻¹	S_{33}^E pPa ⁻¹	S_{44}^E pPa ⁻¹	S_{66}^E pPa ⁻¹	d_{15} pC/N	d_{31} pC/N	d_{33} pC/N	$\frac{\epsilon_{33}^S}{\epsilon_0}$	$\frac{\epsilon_{11}^S}{\epsilon_0}$	ρ kg/m ³
17	-6.71	-8.53	23	43.47	47.42	500	-170	425	1130	914	7700

117
118

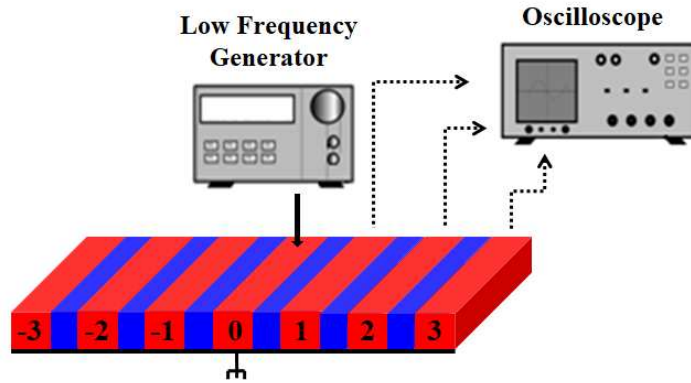
Table I: Physical properties of PZ27 ceramic.

119 **2.2 Crosstalk measurements**

120 Crosstalk measurements are performed on the studied transducer array using two
121 methods as shown in Fig 3 and Fig. 4. In the first technique (Fig. 3), the central element "0" is
122 excited using Agilent 33250A Low Frequency Generator delivering an electrical sine signal V_0 .
123 The neighboring elements "1", "-1", "2", "-2", "3" and "-3" are connected individually to a
124 digital oscilloscope, displaying the parasitic voltage generated on each element (V_i , $i = 1, -1, 2,$
125 $2, 3,$ and -3). In the literature [11, 14] the crosstalk level C (dB) is evaluated from the
126 measurements using the relation (1):

127
$$C(\text{dB}) = 20 \text{Log}\left(\frac{V_i}{V_0}\right), \quad (1)$$

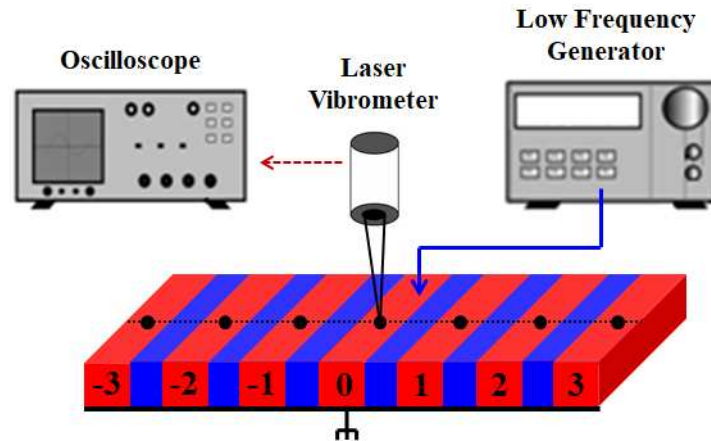
128 This definition considers one element of the studied transducer array as electrically driven,
129 while its neighboring elements are electrically in Open-Circuit (not grounded). In this paper, a
130 second method is proposed to evaluate the crosstalk level when the neighboring elements are
131 connected to the ground, as in the case of the crosstalk's active cancellation methods [16, 24,
132 25, 26, 27]. In this situation, voltage measurement cannot be utilized because the elements are
133 not in Open-Circuit as suggested by the definition (Fig.3).



134
135

Figure 3: Crosstalk's evaluation using voltage measurements.

136 Another solution is to utilize the displacement measurements instead of the voltage ones
 137 as shown in Fig. 4. One of the objectives of this research work is to test the validity of this
 138 method and to evaluate its limitations. For this purpose, displacement measurements are
 139 carried out in the middle of the fabricated array elements using a Polytech psv400 laser
 140 vibrometer (Fig. 4). The results obtained using both methods (Fig. 3 and 4) are compared
 141 numerically and experimentally in the frequency domain.



142

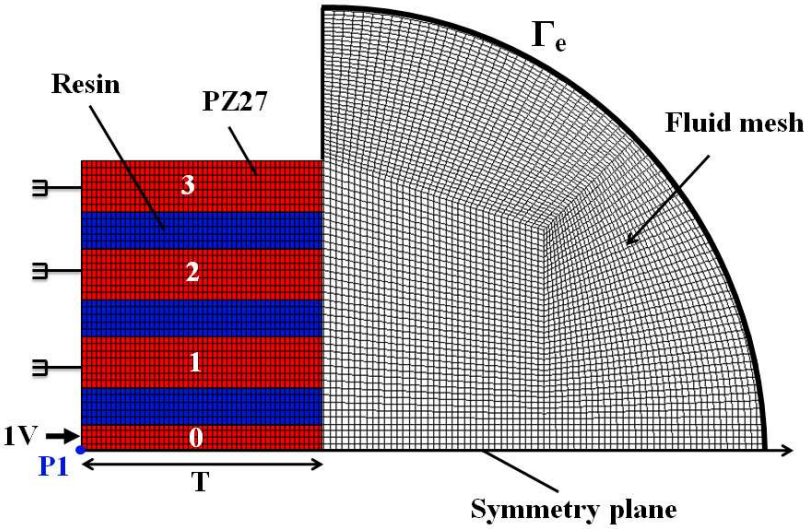
143

Figure 4: Crosstalk's evaluation using displacement measurements.

144 3. Numerical study

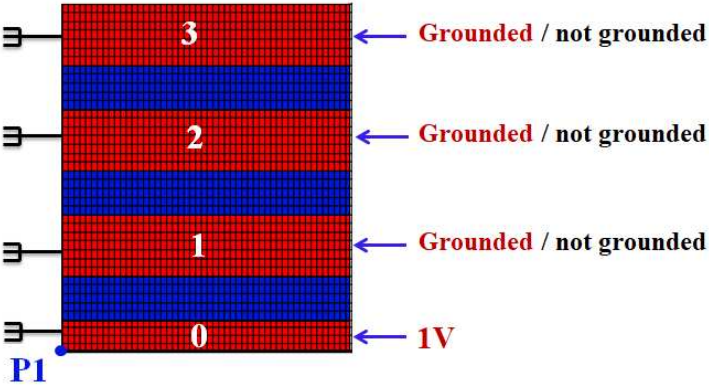
145 The piezoelectric transducer array is first modeled numerically using the ATILA code
 146 (FEM code for elastic and piezoelectric structures radiating in fluid) [28] to determine its
 147 Transmitting Voltage Response (TVR) and to predict the normal displacement at the radiating
 148 surface of each array element. The numerical model is also utilized to compute the array's
 149 electrical impedance and to evaluate the crosstalk level. As shown in Fig. 5(a), the studied
 150 array is composed of seven piezoelectric elements made of PZ27 ceramic bounded to each
 151 other by Acrylic PLEXCIL resin (filling material). Both the piezoelectric array elements and
 152 the filling material (resin) are meshed using isoparametric quadratic elements respecting the
 153 $\lambda/4$ criterion, i.e. the piezoelectric array elements are divided into seven elements along their
 154 width W and fifty elements along their thickness T , whereas the resin elements are divided into
 155 five elements along their width and fifty elements along their thickness. The spacing between
 156 the array elements (d) is chosen equal to 1.2 mm to respect the Nyquist criterion and to avoid
 157 grating lobes. Each element of the studied array has a thickness $T = 3.3$ mm, a width $W = 0.7$
 158 mm and its length is chosen to be 37 mm long, with a Length-to-Thickness Ratio (L/T) of
 159 about 11.21, thus this length can be considered as infinite and a plane strain approximation

160 assumed. In the literature, it is demonstrated that a dominant thickness mode is obtained when
 161 the width-to-thickness ratio W / T is less than or equal to 0.5 [29-30]. This aspect ratio is
 162 chosen about 0.21 to enable the separation of the thickness mode about the undesirable lateral
 163 modes (width and length modes). Furthermore, in our previous work (ref. 8), it was also
 164 demonstrated numerically and experimentally that the influence and the contribution of these
 165 undesirable modes (width and length modes) is negligible. The transducer array radiates in a
 166 fluid medium (water in medical imaging applications) meshed with isoparametric quadratic
 167 elements respecting the $\lambda/4$ criterion. This medium is limited by a non-reflecting surface Γ_e
 168 made up of dipolar elements that absorb the outgoing acoustic wave almost completely [15].
 169 Furthermore, only half the domain is meshed due to symmetry.



170
 171

(a) Structure's mesh.



172
 173

(b) Electrical limit conditions.

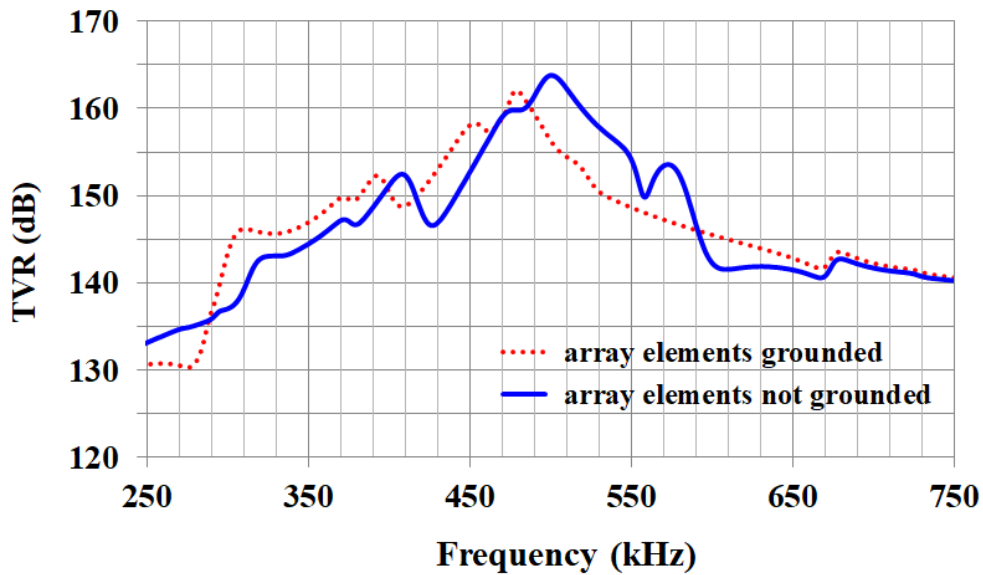
174 **Figure 5:** Schematic description of a seven-element transducer array radiating in water.

175 To study the effects of the electrical limit conditions on the array’s electromechanical
176 behavior, two limit conditions are considered (Fig. 5(b)):

- 177 i) The array’s central element “0” is driven, while its neighboring elements “1”, “2” and “3”
178 are grounded.
- 179 ii) The central element “0” is driven and its neighboring elements “1”, “2” and “3” are not
180 grounded (open-circuit).

181 3.1 Transmitting Voltage Response (TVR)

182 Firstly, the Transmitting Voltage Response (TVR) of the seven-element transducer
183 array is computed between 250 kHz and 750 kHz, for a relative reference pressure $1 \mu\text{Pa} / \text{V}$
184 at 1 m. Fig. 6 compares the TVR obtained considering the electrical limit conditions (i) and
185 (ii). After analysis, it is observed that the two curves follow relatively the same variation, i.e.
186 the same maximums and minimums. Nevertheless, a frequency shift about 20 kHz is obtained
187 between the curves. Furthermore, a parasitic mode (maximum of TVR) is observed around the
188 frequency of 570 kHz, in the curve corresponding to the limit condition (ii). Finally, the
189 maximum of TVR obtained for the limit condition (i) is somewhat less than that computed for
190 the condition (ii) (about 2 dB).

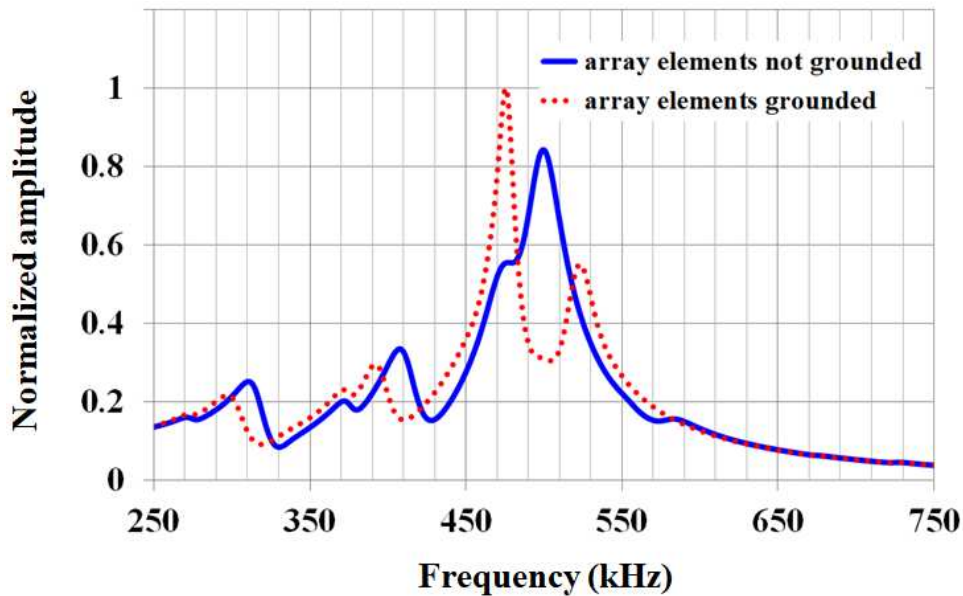


191
192 **Figure 6:** Transmitting Voltage Response (TVR) of the seven-element transducer array.

193 3.2 Displacement

194 The normal displacement is also computed in the middle of the radiating surface of the
195 central element “0”, i.e. at the position P1 (Fig. 5b) between 250 kHz and 750 kHz. Fig. 7

196 compares the normalized displacement curves (all values are divided by the maximum value
 197 reached by one of the compared curves) obtained considering the electrical limit conditions (i)
 198 and (ii). It is observed from this figure that the results are different, particularly between 450
 199 kHz and 550 kHz. In this frequency domain, a maximum of displacement is obtained around
 200 500 kHz (mechanical resonant frequency), for the limit condition (ii). Whereas, in the case of
 201 the limit condition (i), two resonance frequencies 475 kHz and 520 kHz are obtained. Finally,
 202 the comparison of the two curves indicates a frequency shift (about 25 kHz) between the two
 203 displacement peaks observed in the frequency band 450 kHz – 550 kHz.

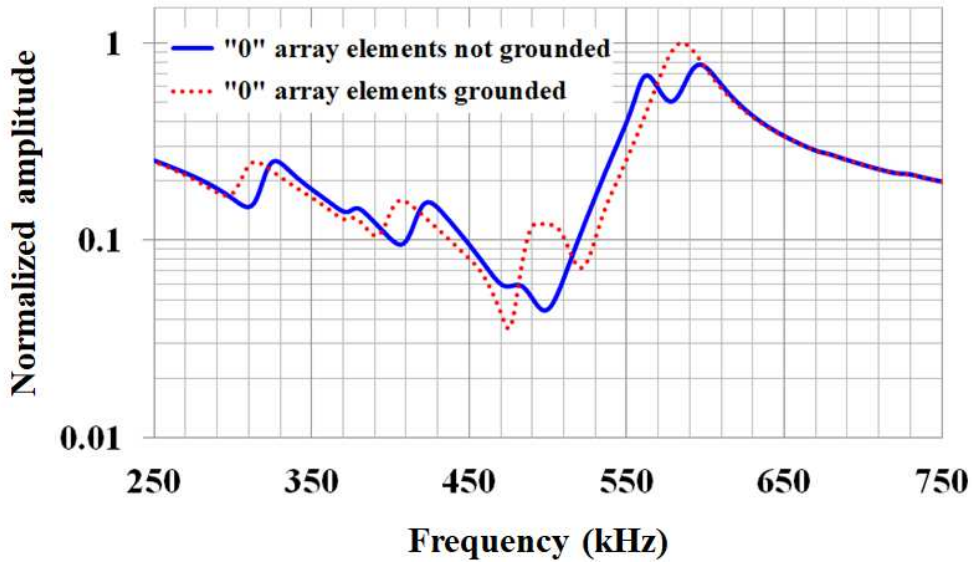


204
 205 **Figure 7:** Normal displacement computed at the radiating surface of the element “0”.

206 **3.3 Electrical impedance**

207 To observe the effect of the limit conditions (i) and (ii) on the electrical behavior of the
 208 transducer array, the electrical impedances computed using the numerical model are
 209 compared in the frequency domain 250 kHz – 750 kHz, as shown in Fig. 8. After analysis, it
 210 is observed that the two curves follow the same behavior in the frequency domains 250 kHz –
 211 470 kHz and 590 kHz – 750 kHz. Nevertheless, a frequency shift (about 20 kHz) is obtained
 212 between the two curves in the first frequency band. The major differences are observed
 213 around the thickness mode, i.e. in the frequency band 470 kHz – 590 kHz. In this domain, two
 214 resonance frequencies (475 kHz and 520 kHz) and a one anti-resonance frequency (581 kHz)
 215 are obtained for the limit condition (i), whereas in the case of the condition (ii), one resonant
 216 frequency is obtained at about 500 kHz and two anti-resonance frequencies are observed at
 217 571 kHz and 595 kHz. As seen previously in Fig. 7, the resonance frequencies (minimum of

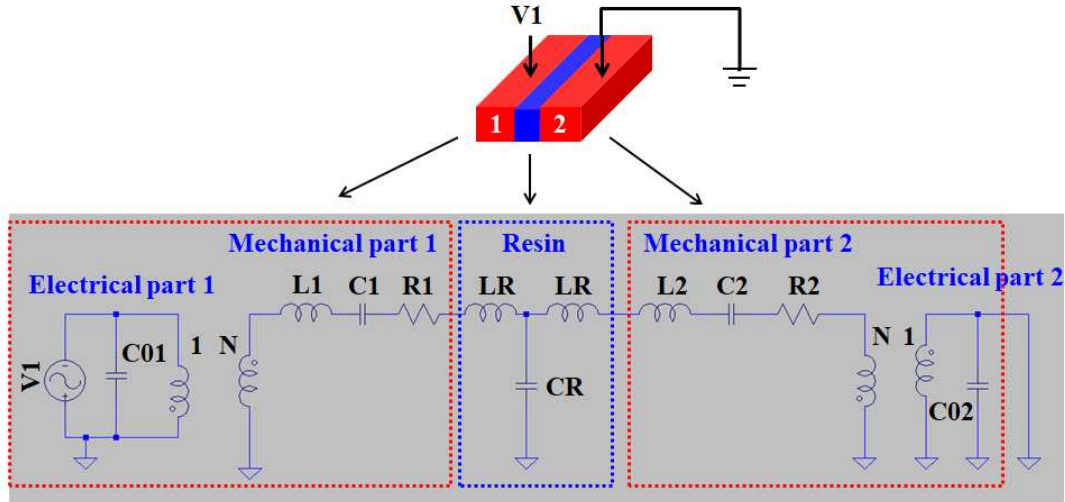
218 impedance) correspond also to the mechanical resonance frequencies (maximum of
 219 displacement).



220
 221 **Figure 8:** Numerical electrical impedance of the central element “0”.

222
 223 The differences between the results obtained under the limit conditions (i) and (ii), i.e.
 224 TVR, displacement and impedance curves, can be explained by the simplified equivalent
 225 circuit represented in Fig. 9. In this case, only two piezoelectric elements bonded to each
 226 other by a non-conductive resin are considered, i.e. an active piezoelectric element (part 1)
 227 and its neighbouring element grounded or in open-circuit (part 2). The piezoelectric elements
 228 are represented by their equivalent electromechanical circuit composed of an electrical part
 229 ($R_{01,2}$, $C_{01,2}$) and a mechanical part ($R_{1,2}$, $L_{1,2}$ and $C_{1,2}$). The elements $R_{1,2}$, $L_{1,2}$ and $C_{1,2}$
 230 correspond to a mass - spring system, for which $R_{1,2}$ represents the mechanical dissipations,
 231 $L_{1,2}$ the mass and $C_{1,2}$ the compliance (flexibility) of the material. $R_{01,2}$ and $C_{01,2}$ represent the
 232 dielectric losses and the static capacitance of the piezoelectric material. The two parts are
 233 connected by a transformer converting the electrical energy to mechanical energy and vice-
 234 versa and having a transformation ratio N . Because of their very large value (several $M\Omega$), the
 235 resistors $R_{01,2}$ are neglected. In the same manner, the non-conductive resin is represented by its
 236 equivalent circuit (L_R , C_R). In our previous work [7], it was demonstrated that this
 237 representation is more accurate in the vicinity of the considered resonant frequency (thickness
 238 resonance). According to the equivalent circuit, it is clear that when the element 2 is
 239 grounded, its static capacitance C_{02} is short-circuited, i.e. the contribution of the electrical
 240 branch (C_{02}) is suppressed. Consequently, only the mechanical branch (R_2 , L_2 and C_2)
 241 contributes to the total electrical impedance of the structure composed of the elements 1 and

242 2. Finally, in the case of the transducer array composed of seven piezoelectric elements, the
 243 limit condition (i) is responsible in the elimination of the individual static capacitances and it
 244 results in non-negligible differences between the curves obtained under the limit conditions (i)
 245 and (ii), e.g. the observed frequency shifts.



246
 247 **Figure 9:** Equivalent circuit of two piezoelectric elements bonded to each other by resin.

248 **3.4 Crosstalk**

249 The crosstalk level is firstly evaluated at the two characteristic frequencies (maximum
 250 of displacement) 475 kHz and 520 kHz using both methods. The estimation of the crosstalk
 251 level C utilizes the conventional method (relation (1)) when the neighboring elements are not
 252 grounded (limit condition (ii)). In the case of the limit condition (i) (neighboring elements
 253 grounded) the proposed method is to evaluate the crosstalk from the displacement values in
 254 the middle of the array elements) using the relation (2):

255
$$C(\text{dB}) = 20 \text{Log}\left(\frac{u_i}{u_0}\right), \quad (2)$$

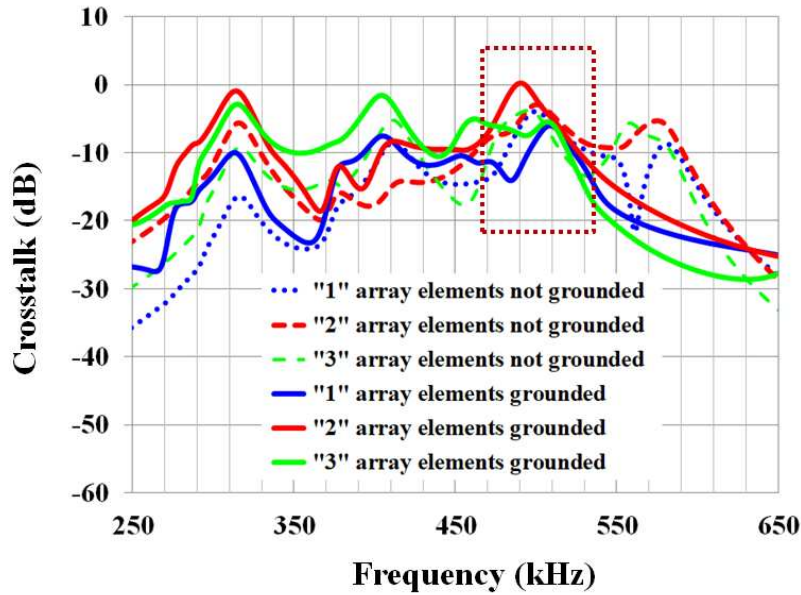
256 where u_0 represents the normal displacement computed in the middle of the central
 257 element "0" and u_i ($i = 1, 2, 3$) the displacement in the middle of the neighboring elements
 258 "1", "2" and "3". The results obtained using the two methods are summarized in Table II. The
 259 comparison shows that the two methods, i.e. evaluation of crosstalk level by the relation (1)
 260 and using parasitic displacements instead of voltages C_u (relation 2), give relatively similar
 261 crosstalk values at the resonance frequencies. The difference (about 1 dB) is probably because
 262 the definition of the crosstalk is based on the voltage, which is an average value, whereas, the
 263 displacement's method is punctual (obtained in the middle of the elements).

Element	"1"	"2"	"3"
Crosstalk C_u (dB)	-11.8	-5.2	-6.1
	-8.8	-7.9	-10
Crosstalk C (dB)	-12.7	-7.4	-7.7
	-8.1	-6.7	-11.1

264

265 **Table II:** Crosstalk evaluated at the resonance frequencies 475 kHz and 520 kHz (bold values).

266 The comparison is then extended to a large frequency band between 250 kHz and 650
 267 kHz, as shown in Fig. 10. After analysis, it is observed that the crosstalk evaluated using both
 268 methods are similar around the two characteristic frequencies (see dashed rectangular). The
 269 difference between the two curves increases beyond the resonance frequencies. In other
 270 words, the crosstalk evaluated using the displacement in the middle of the array elements is a
 271 good approximation in the vicinity of the considered mode (thickness mode in this work).



272

273 **Figure 10:** Crosstalk computed using relation 1 (array elements not grounded) compared to
 274 that obtained from the relation 2 (array elements grounded).

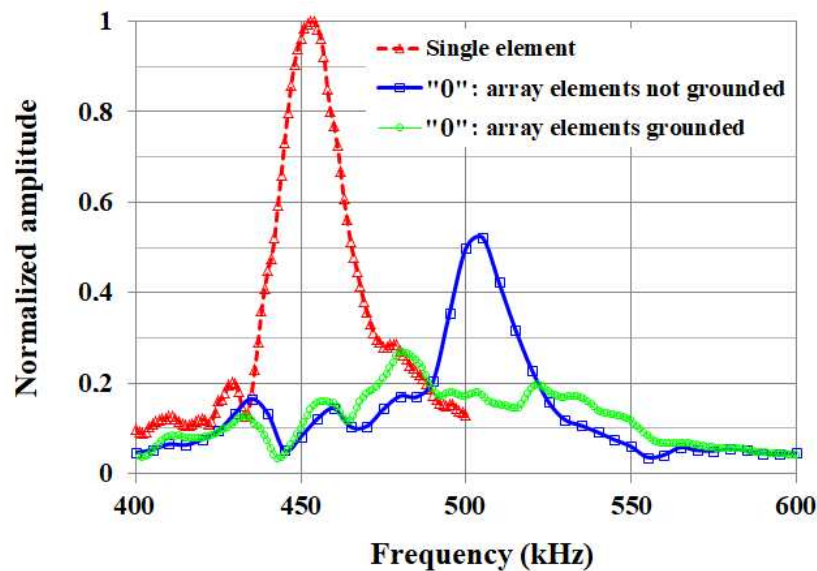
275 4. Experimental Characterization

276 The manufactured transducer array (Fig. 2), is characterized experimentally by electrical
 277 impedance and displacement measurements, in both conditions (i) and (ii). The crosstalk level

278 is also evaluated using the previous methods, i.e. from the parasitic voltages (relation (1)) and
 279 using the proposed displacements method (relation (2)). For the sake of simplification,
 280 measurements are realized in air. The results are then compared to those obtained numerically
 281 in the air medium instead of water. It is important to notice that the FEM calculations are first
 282 done in the water medium (section 3) to see the effects of the limit conditions on the
 283 transducer arrays utilized in medical imaging, and then done in the air medium to compare the
 284 numerical results with the experimental ones.

285 4.1 Displacement

286 To avoid the edge effects, displacement measurements are realized in the middle of the
 287 central element “0” using a Polytech OFV353 Laser Vibrometer. The curves obtained in both
 288 conditions (i) and (ii) are compared with that measured in the middle of a single element (Fig.
 289 11).

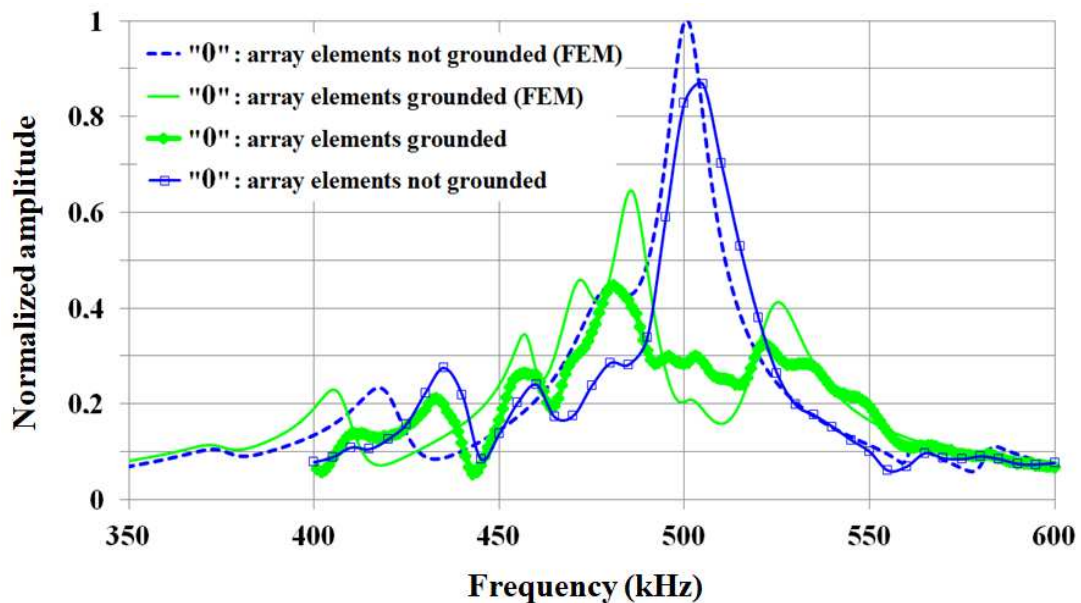


290
 291 **Figure 11:** Normalized displacement amplitude measured in the middle of the central element
 292 “0” compared to that obtained in the middle of a single piezoelectric element.
 293

294 As expected, the curves measured on the element “0” (conditions (i) and (ii)) are
 295 different, particularly in the frequency band 450 kHz - 550 kHz. In this domain, the
 296 maximum displacement is obtained at about 500 kHz for the condition (ii). Whereas, in the
 297 case of the condition (i), two mechanical resonance frequencies 481 kHz and 520 kHz are
 298 obtained. Furthermore, the displacement amplitudes at both frequencies are lower than those
 299 observed at 500 kHz. Finally, a frequency shift is obtained between the single element’s
 300 resonance frequency (452 kHz) and the array’s resonance frequencies. This result is due to the

301 presence of the neighboring elements, which shifts the resonance frequencies towards the high
302 frequencies and reduces the amplitude of the displacement, e.g. the maximum displacement
303 for the condition (ii) is about half that obtained in the case of the single element.

304 Fig. 12 compares the displacements measured in the middle of the element “1”, in both
305 conditions (i) and (ii) to the numerical results (FEM). It is seen from this figure that the results
306 obtained are similar. Nevertheless, a small frequency shift is observed between the curves
307 (about 4 kHz), due to the materials’ incertitude. Furthermore, the displacement’s amplitude
308 obtained numerically is relatively high compared to the measured one, because the resin’s real
309 losses are not taken into account (about 5%) and the piezoelectric material losses are not
310 considered.

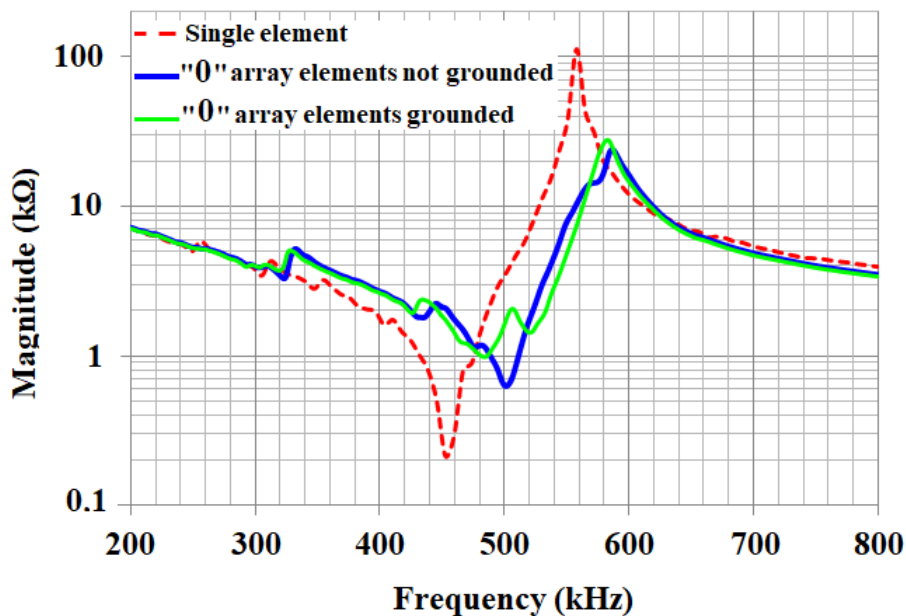


311
312 **Figure 12:** Normalized displacements amplitude measured in the middle of the central
313 element “0” compared to the numerical results (FEM).
314

315 4.2 Electrical impedance

316 The electrical impedance of the transducer array is also measured in the frequency band
317 200 kHz – 800 kHz. Fig. 13 compares the curves obtained considering the limit conditions (i)
318 and (ii). To show the effects of the interactions between the array elements (crosstalk), the
319 transducer array’s curves are also compared to that of a single piezoelectric element. After
320 analysis, different conclusions can be made. Firstly, concerning the single element, a
321 minimum and a maximum of impedance are observed at 452 kHz and 558 kHz respectively.
322 Secondly, a frequency shift can be observed between the transducer array curves and the

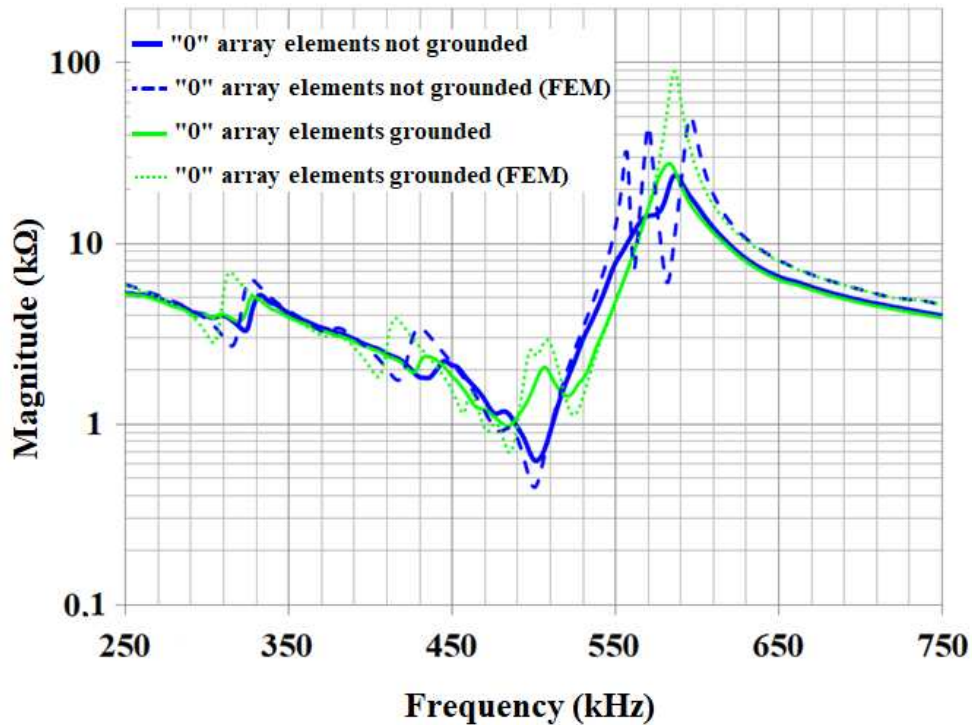
323 electrical impedance of the single element (about 30 kHz). This result is due to the presence
 324 of the neighboring piezoelectric elements, which shifts the resonance and anti-resonance
 325 frequencies towards the high frequencies. Furthermore, due to the crosstalk phenomenon,
 326 parasitic vibrations are obtained around the array's resonance (condition (i)) and anti-
 327 resonance frequencies (condition (ii)), contrary to the single piezoelectric element. Finally, in
 328 the same manner as the numerical results, differences are observed between the electrical
 329 impedance curves obtained in the case of the conditions (i) and (ii). Indeed, two resonance
 330 frequencies (481 kHz and 520 kHz) and a one anti-resonance frequency (580 kHz) are
 331 obtained in the case of the condition (i), whereas in the case of the condition (ii), a one
 332 resonance frequency is obtained at 500 kHz and two anti-resonance frequencies are observed
 333 at 565 kHz and 583 kHz. As seen in Fig. 11, the resonance frequencies (minimum of
 334 impedance) correspond also to the mechanical resonance frequencies (maximum of
 335 displacement).



336
 337 **Figure 13:** Experimental electrical impedance of the element “0” compared to that of a single
 338 piezoelectric element (dashed line).
 339

340 Fig. 14 compares the experimental and numerical (FEM) electrical impedances in both
 341 conditions (i) and (ii): array elements grounded and not grounded. It is seen from this figure
 342 that the results obtained are similar. Nevertheless, a small frequency shift is observed between
 343 the curves in the frequency band 250 kHz – 450 kHz, due to the materials' incertitude.
 344 Furthermore, in the case of the condition (ii), i.e. when the central element “1” is excited and
 345 its neighboring elements are grounded, only two anti-resonance frequencies are observed in

346 the measured curve, instead of three frequencies as obtained numerically. This result is mainly
 347 due to the resin losses chosen in the numerical model (about 5 %) and the piezoelectric
 348 material losses, which are not taken into account.



349
 350 **Figure 14:** Electrical impedance measured on the element “0” compared to the numerical one.

351 **4.3 Crosstalk**

352 The experimental setup presented previously in Fig. 3 is first utilized to measure the
 353 parasitic voltages generated on the neighboring elements “1”, “-1”, “2”, “-2”, “3”, and “-3”,
 354 when the central element “0” is excited by a harmonic signal having 10 V amplitude. In this
 355 case, measurements are realized at the first resonant frequency of 481 kHz. The crosstalk
 356 level C (dB) is then evaluated using the relation (1). The obtained results are given in Table
 357 III.

358

Element	“-3”	“-2”	“-1”	“0”	“1”	“2”	“3”
Voltage (V)	5.04	1.64	3.23	10	2.73	1.62	4.47
Crosstalk C (dB)	-5.95	-15.7	-9.81	0	-11.28	-15.81	-7

359

360

Table III: Crosstalk evaluated using parasitic voltages.

361 The measurements show that when the central element “0” is excited, it vibrates mainly
362 in its thickness mode, but it generates significant undesirable voltages on its passive
363 neighboring elements “1”, “-1”, “2”, “-2”, “3” and “-3”. These results demonstrate the
364 presence of crosstalk in the fabricated transducer array, i.e. the measured average values about
365 -10.54 dB, -15.75 dB, and -6.47 dB on the first, second and third neighboring elements
366 respectively. Furthermore, a high level of crosstalk is noticed in the case of the third
367 neighboring elements “3” and “-3” due to edge effects. As explained previously, in the case of
368 active cancellation of crosstalk, the determination of the correction voltages considers the
369 neighboring elements electrically in Short-Circuit (condition (i)). In this situation, the
370 crosstalk cannot be estimated using the conventional definition (relation (1)). The proposed
371 solution to evaluate the crosstalk level is to measure the parasitic displacements generated on
372 the neighboring elements using the experimental setup given in Fig. 4 and then deduce the
373 crosstalk C_u (dB) from the relation (2). In this case, the results obtained when the central
374 element “0” is excited (at the frequency 481 kHz) and its neighboring elements are connected
375 to the ground (Fig. 4) are summarized in Table IV. In the same manner as the previous results
376 (Table III), significant parasitic displacements are observed on the passive neighboring
377 elements. Consequently, strong crosstalk is noticed on the first (“1”, “-1”) and third (“3”, “-
378 3”) neighboring elements particularly.

Element	“-3”	“-2”	“-1”	“0”	“1”	“2”	“3”
Displacement (nm)	6.21	2.73	5.48	11.8	3.62	1.8	5.59
Crosstalk C_u(dB)	-5.58	-12.71	-6.66	0	-10.26	-16.33	-6.49

379

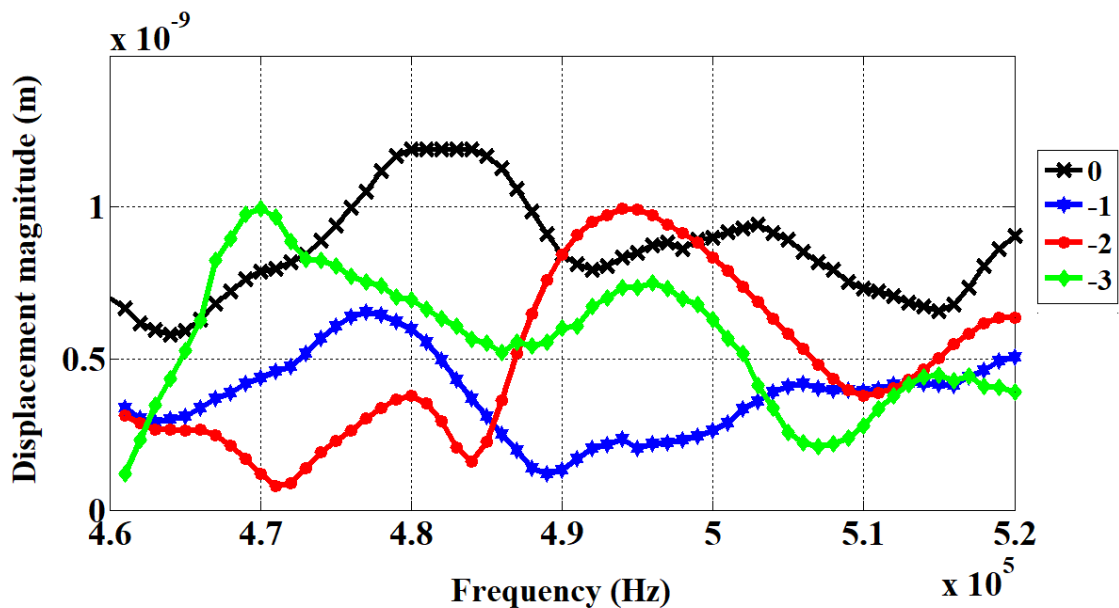
380

Table IV: Crosstalk evaluated using parasitic displacements.

381 The comparison of the results given in Tables III and IV shows that the two methods,
382 i.e. estimation of the crosstalk level by the relation (1) and using parasitic displacements
383 instead of voltages, give relatively similar crosstalk values at the resonant frequency. The
384 difference is because the definition of the crosstalk is based on the voltage, which is an
385 average value, whereas, the displacement’s method is punctual, i.e. measurements are realized
386 only in the middle of the transducer array elements (Fig. 4), to avoid edge effects. In other
387 words, this method supposes the displacement uniform at the surface of the individual
388 elements, which is not true. For more precision, it would be better to measure the
389 displacement at the whole surface of the array elements, to take into account the contribution

390 of the parasitic length mode [8, 16]. The latter makes the displacement not uniform.
 391 Measurements can be achieved with a Scanning Laser Vibrometer, e.g. Polytech psv400. In
 392 this situation, average displacement values can be obtained and the precision of crosstalk
 393 evaluation can be improved.

394 To estimate the crosstalk level in a relatively large frequency band (460 kHz – 520 kHz)
 395 using the relation (2), displacement measurements are first done in the middle of the array
 396 elements. The results obtained on the elements “0”, “-1”, “-2”, and “-3”, when the central
 397 element “0” is excited by a harmonic signal having 1V amplitude and its neighboring
 398 elements are grounded (limit condition (i)) are shown in Fig. 15. After analysis, it is observed
 399 that significant parasitic displacements are obtained on the passive neighboring elements due
 400 to the crosstalk phenomenon. At the resonant frequency 481 kHz, a maximum of
 401 displacement is measured on the central element “0” ($u_0 = 1.19$ nm). The parasitic
 402 displacements measured on the element “-1”, “-2” and “-3” are about 46 %, 25 % and 56 %
 403 the amplitude of the excited element “0” respectively.



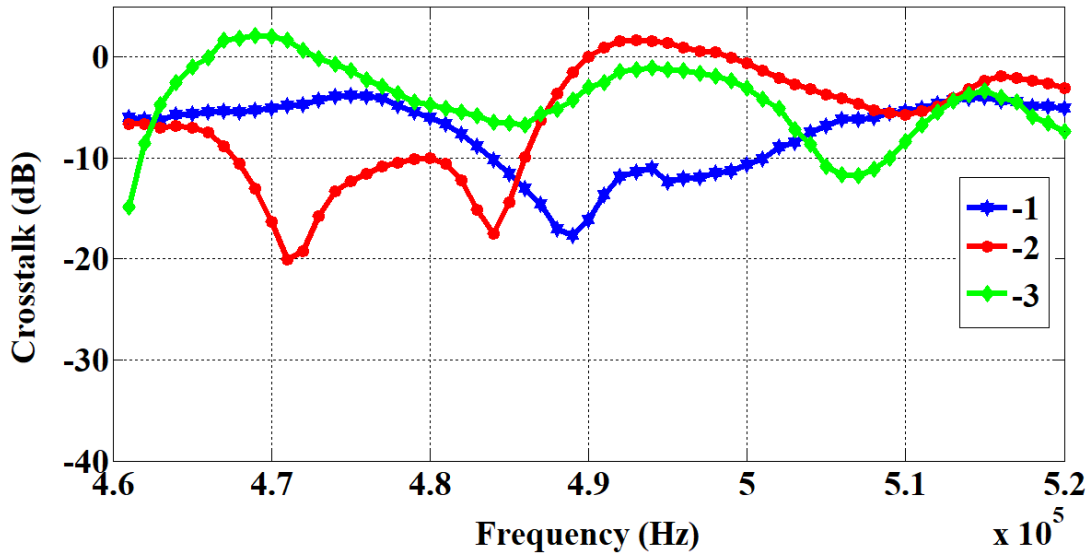
404

405 **Figure 15:** Displacement measured in the middle of the array elements “0”, “-1”, “-2” and “-
 406 3”, when the central element “0” is excited by a harmonic signal having 1V
 407 amplitude and its neighboring elements grounded.

408

409 The relation (2) is then utilized to evaluate the crosstalk level in terms of displacement
 410 as shown in Fig. 16. According to the latter, it is clear that in the frequency band 460 kHz –
 411 520 kHz, the transducer array presents a strong crosstalk level (greater than -20 dB). Around
 412 the central element’s resonant frequency 481 kHz, i.e. between 475 kHz – 487 kHz, the

413 highest crosstalk level is obtained for the third element “-3”, located on the array’s edge. In
 414 the same frequency band, a relatively similar crosstalk level is measured on the first “-1”.
 415 Finally, the crosstalk level observed of the second neighbor “-2” is also not negligible (higher
 416 than -20 dB). Because of these high crosstalk levels, active crosstalk cancellation methods are
 417 successfully proposed and utilized to reduce the interactions between the array elements
 418 (crosstalk) and to improve its performance [16, 27].



419
 420 **Figure 16:** Crosstalk estimated on the array elements “-1”, “-2” and “-3” by using the relation
 421 2 (array elements grounded).
 422

423 5. Conclusion

424 In this paper, the effects of the electrical limit conditions on the electromechanical
 425 behavior of a piezoelectric transducer array are investigated numerically and experimentally.
 426 A seven-element transducer array radiating in water is first modeled using the 2D Finite
 427 Element Method. Globally, the computed results (TVR, electrical impedance and
 428 displacement) indicated that the influence of the limit conditions (central element’s
 429 neighboring elements grounded or not) is mainly observed around the thickness mode’s
 430 resonance and anti-resonance frequencies. Furthermore, a frequency shift is obtained between
 431 the curves computed considering the two limit conditions (about 20 kHz). However,
 432 concerning the crosstalk, it is shown that the values calculated under the two electrical limit
 433 conditions are relatively similar (about 1 dB of difference) at the mechanical resonance
 434 frequencies (maximum of displacement) 475 kHz and 520 kHz. The difference between the
 435 computed curves increases beyond the resonance frequencies. The numerical results

436 (electrical impedance and displacements) computed in the air medium are successfully
437 compared to those measured using an impedance analyzer and a Laser Vibrometer
438 respectively. In both cases, it is shown that the influence of the limit conditions is mainly
439 observed around the thickness mode's resonance and anti-resonance frequencies.
440 Furthermore, the crosstalk level is evaluated experimentally at the mechanical resonance
441 frequency 481 kHz using two methods, i.e. voltage and displacement measurements. The
442 results obtained are relatively similar. Nevertheless, for more precision, a Scanning Laser
443 Vibrometer should be utilized to achieve average displacement values instead of punctual
444 ones. Finally, the crosstalk level is estimated in the frequency band 460 kHz – 520 kHz using
445 the proposed method, i.e. deduced from punctual displacement measurement. According to
446 the results, the manufactured seven-element transducer array presents a strong crosstalk level
447 (greater than -20 dB), which should be reduced to improve the array's electromechanical
448 behavior. For this purpose, active crosstalk cancellation methods can be utilized, i.e. the
449 application of adequate correction voltages to the array elements can be a solution to reduce
450 the crosstalk level. Dicing the inter-element filling material can also contribute to reduction of
451 this undesirable phenomenon (crosstalk).

452 **References**

- 453 [1] W. Lee and Y. Roh, "Ultrasonic transducers for medical diagnostic imaging," *Biomedical*
454 *Engineering Letters*, 7(2):91–97, 2017.
- 455 [2] B. Cox, and P. Beard, "Imaging Techniques: Super-Resolution Ultrasound," *Nature*,
456 527(7579):451–452, 2015.
- 457 [3] X. Jiang, S. Li, J. Kim, J. Ma, W. Huang, and X. Jian, "High Frequency Piezo-Composite
458 Micromachined Ultrasound Transducer Array Technology for Biomedical Imaging,"
459 *ASME Biomedical and Nanomedical Technologies Concise Monograph Series*, ASME
460 Press, New York, 2017.
- 461 [4] P. Anastasiadis, A. Mohammadabadi, M. J. Fishman, J. A. Smith, B. A. Nguyen,
462 D. S. Hersh, and V. Frenkel, "Design, characterization and evaluation of a laser-guided
463 focused ultrasound system for preclinical investigations," *BioMedical Engineering*
464 *OnLine*, 18(1):36, 2019.
- 465 [5] D. S. Hersh, P. Anastasiadis, A. Mohammadabadi, B. A. Nguyen, S. Guo, J. A. Winkles,
466 A. J. Kim, R. Gullapalli, A. Keller, V. Frenkel, and G. F. Woodworth, "MR-guided
467 transcranial focused ultrasound safely enhances interstitial dispersion of large polymeric
468 nanoparticles in the living brain," *PLOS ONE*, 13(2):e0192240, 2018.
- 469 [6] Y. Roh and M. S. Afzal, "Optimal design of a sparse planar array transducer for
470 underwater vehicles by inclusion of crosstalk effect," *Japanese Journal of Applied*
471 *Physics*, 57(7S1):07LG02-1–07LG02-7, 2018.

- 472 [7] A. Bybi, O. Mouhat, M. Garoum, H. Drissi, and S. Grondel, "One-dimensional equivalent
473 circuit for ultrasonic transducer arrays," *Applied Acoustics*, 156:246–257, 2019.
- 474 [8] A. Bybi, D. Khouili, C. Granger, M. Garoum, A. Mzerd, and A.-C. Hladky-Hennion,
475 "Experimental Characterization of A Piezoelectric Transducer Array Taking into Account
476 Crosstalk Phenomenon," *International Journal of Engineering and Technology
477 Innovation*, 10(1):01–14, 2020.
- 478 [9] M. Celmer, K. J. Opielinski, and M. Dopierala, "Structural model of standard ultrasonic
479 transducer array developed for FEM analysis of mechanical crosstalk," *Ultrasonics*,
480 83:114–119, 2018.
- 481 [10] J. Henneberg, A. Gerlach, H. Storck, H. Cebulla, and S. Marburg, "Reducing mechanical
482 cross-coupling in phased array transducers using stop band material as backing," *Journal
483 of Sound and Vibration*, 424:352–364, 2018.
- 484 [11] K. J. Opielinski, M. Celmer, and R. Bolejko, "Crosstalk effect in medical ultrasound
485 tomography imaging," In *Joint Conference-Acoustics*, pp. 1-6, 2018.
- 486 [12] S. Pyo and Y. Roh, "Analysis of the crosstalk in an underwater planar array transducer
487 by the equivalent circuit method," *Japanese Journal of Applied Physics*,
488 56(7S1):07JG01-1–07JG01-6, 2017.
- 489 [13] W. Lee and Y. Roh, "Optimal design of a piezoelectric 2D array transducer to minimize
490 the cross-talk between active elements," In *IEEE Ultrasonics Symposium (IUS)*, pp.
491 2738-2741, 2009.
- 492 [14] I. S. Domínguez, P. A. Contla, E. M. Hernández, and M. Antônio von Krüger, "Crosstalk
493 effects caused by the geometry of piezoelectric elements in matrix ultrasonic
494 transducers," *Revista Brasileira de Engenharia Biomédica*, 27(2):90–97, 2011.
- 495 [15] J. Assaad and C. Bruneel, "Radiation from finite phased and focused linear array
496 including interaction," *The Journal of the Acoustical Society of America*, 101(4):1859–
497 1867, 1997.
- 498 [16] A. Bybi, S. Grondel, A. Mzerd, C. Granger, M. Garoum, and J. Assaad, "Investigation of
499 cross-coupling in piezoelectric transducer arrays and correction," *International Journal of
500 Engineering and Technology Innovation*, 9(4):287–301, 2019.
- 501 [17] F. P. Branca, F. Bini, F. Marinozzi, and A. Grandoni, "Optimum choice of acoustic
502 properties of filling materials using optical measurement," In *IEEE Ultrasonics
503 Symposium (IUS)*, pp. 1663-1665, 2004.
- 504 [18] W. Lee and Y. Roh, "Optimal design of a piezoelectric 2D array transducer to minimize
505 the cross-talk between active elements," In *IEEE Ultrasonics Symposium (IUS)*, pp.
506 2738-2741, 2009.
- 507 [19] H. J. Fang, Y. Chen, C. M. Wong, W. B. Qiu, H. L. Chan, J. Y. Dai, Q. Li, and Q. F.
508 Yan, "Anodic aluminum oxide-epoxy composite acoustic matching layers for ultrasonic
509 transducer application," *Ultrasonics*, 70:29–33, 2016.
- 510 [20] M. H. Amini, T. W. Coyle, and T. Sinclair, "Porous ceramics as backing element for
511 high-temperature transducers," *IEEE Transactions on Ultrasonics, Ferroelectrics, and
512 Frequency Control*, 62(2):360–372, 2015.

- 513 [21] S. M. Ji, J. H. Sung, C. Y. Park, and J. S. Jeong, "Phase-canceled backing structure for
514 lightweight ultrasonic transducer," *Sensors and Actuators A: Physical*, 260:161–168,
515 2017.
- 516 [22] K. C. T. Nguyen, L. H. Le, M. D. Sacchi, L. Q. Huynh, and E. Lou, "Adaptive noise
517 cancellation in the intercept times-slowness domain for eliminating ultrasonic crosstalk in
518 a transducer array," In *Proc. IFMBE, 5th International Conference on Biomedical
519 Engineering in Vietnam*, Springer, vol. 46, pp. 32-35, 2015.
- 520 [23] C. Ishihara, T. Ikedaa, and H. Masuzawaa, "Higher-frame-rate ultrasound imaging with
521 reduced cross-talk by combining a synthetic aperture and spatial coded excitation," In
522 *Proc. SPIE, Medical Imaging, Ultrasonic Imaging and Tomography*, vol. 9790, pp.
523 97901Z-1-97901Z-7, 2016.
- 524 [24] B. Cugnet, A.-C. Hladky, and J. Assaad, "Numerical technique to reduce crosscoupling
525 in acoustical arrays," *Ultrasonics*, 40:503–506, 2002.
- 526 [25] S. Zhou, G. L. Wojcik, and J. A. Hossack, "An approach for reducing adjacent element
527 crosstalk in ultrasound arrays," *IEEE Trans. Ultrason. Ferroelectr. Freq. Contr.*,
528 50(12):1752–1761, 2003.
- 529 [26] S. Zhou, G. L. Wojcik, and J. A. Hossack, "Reducing inter-element acoustic crosstalk in
530 capacitive micromachined ultrasound transducers," *IEEE Trans. Ultrason. Ferroelectr.
531 Freq. Contr.*, 54(6):1217–1228, 2007.
- 532 [27] A. Bybi, C. Granger, S. Grondel, A. C. Hladky -Hennion, and J. Assaad, "Electrical
533 method for crosstalk cancellation in transducer arrays," *NDT & E International*, 62:115-
534 121, 2014.
- 535 [28] ATILA, Finite-Element Software Package for the analysis of 2D & 3D structures based
536 on smart materials Version 6.0.2 User's Manual, November (2010).
- 537 [29] J. Sato, M. Kawabuchi, and A. Fukumoto, "Dependence of electromechanical coupling
538 coefficient on the width-to-thickness ratio plank-shaped piezoelectric transducers used for
539 electronically scanned ultrasound diagnostic systems," *The Journal of the Acoustical
540 Society of America*, 66(6):1609–1611, 1979.
- 541 [30] W. Friedrich, H. Kaarmann, and R. Lerch, "Finite element modeling of acoustic radiation
542 from piezoelectric phased antennas," In *IEEE Ultrasonics Symposium (IUS)*, pp. 763-
543 767, 1990.